ASSESSING POTENTIAL DISRUPTIONS FROM EARTHQUAKES IN THE HISTORICAL PENINSULA IN ISTANBUL USING 3D MODELLING

J. de Vries[1*], F.Atun[1], M.N. Koeva[1]

[1]ITC Faculty Geo-Information Science and Earth Observation, University of Twente, Enschede, the Netherlands - j.devries@student.utwente.nl, (f.atun, m.n.koeva)@utwente.nl

Commission IV, WG10

KEY WORDS: Earthquake, Vulnerability, Risk, Potential disruptions, 3D models

ABSTRACT:

The increased number of city networks such as 100 Resilient Cities, proves the importance of making cities disaster resilient. The major difficulty on this trajectory is the interrelated components in urban systems that influence each other and increase uncertainty in the risk assessment and management. This study analyses the potential disruptions that impact traffic control with the help of multi-hazard risk assessment for the historical peninsula of the city of Istanbul. 3D model is created for the visualisation of disaster risk to support the communication of the causes of such potential disruptions. The additive normalization indicator-based approach is used to assess the socioeconomic, road and systemic vulnerability and risk. Besides, the EMS-98 Macroseismic method is applied to determine the building vulnerability and damage grades. The results show that the socioeconomic vulnerability is high to very high which is likely to contribute to traffic congestions and communication issues. In addition, most of the buildings are expected to be 'very heavily damaged'. So, while roads have low risk to damage, there is high risk for road blockages in the narrow streets of the case study area. The application of 3D models improves the recognition of buildings and the identification of the causes of road blockages.

1. INTRODUCTION

Disasters continue disrupting everyday life, causing economic loss, infrastructural damages and injuries or loss of human life. They create immediate humanitarian crises and negatively affect the socioeconomic development of cities in the long term. The increased number of city networks such as 100 Resilient Cities and Global Resilient City Networks, proves the importance of making cities disaster resilient. The major difficulty on this trajectory is the uncertainty due to the complexity of cities. Meaning that in cities there are many interrelated components such as built-up environment, people, organisations, technology and economy that influence each other. These Interactions aggravate the complexity and impact of disasters and make them hard to predict (Shimizu & Clark, 2015).

Istanbul is a megacity with currently over 15 million inhabitants that are exposed to increased risk of a major earthquakes due to the east to west progression along the North Anatolian Fault (Atun & Menoni, 2014). Experts predict that an earthquake of at least magnitude 7 will strike the city within the next 30 years (35-70% chance) (Ergintav et al., 2014). Next to this, Istanbul has shown to be at risk to the cascading effects of an earthquake such as fire, liquefaction and tsunamis (Alpar et al., 2003; JICA & IMM, 2002). Contributing to the risk that exist in Istanbul are the many vulnerable structures, densely urbanized and populated areas, a great amount of traffic causing traffic jams and the many people from the low socioeconomic groups (Atun & Menoni, 2014). The case study area exists of three neighbourhoods, Sehremini, Topkapi and Molla Gürani, which are located in the historical peninsula of Istanbul, in Fatih Municipality, known to be the heart for tourism and transportation (see Figure 1).

Existing seismic vulnerability and risk assessments maps and plans show the situation in two dimensions. According to

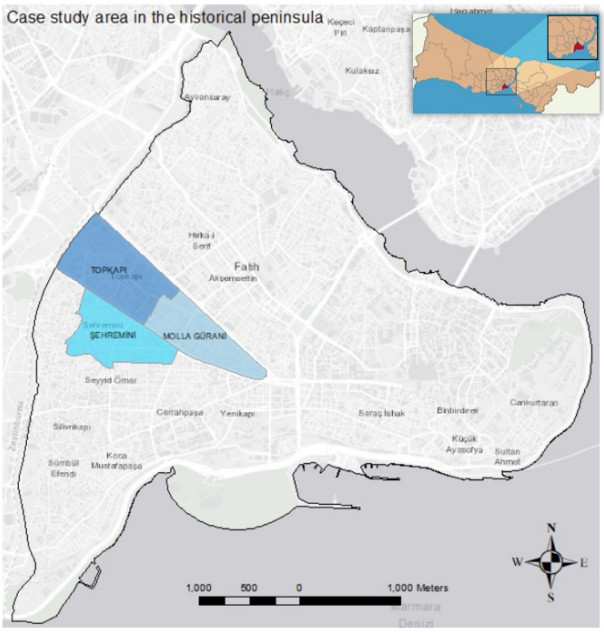

Figure 1. Case study area in Fatih, Istanbul. Sources: de Vries, 2022, and https://en.wikipedia.org/wiki/Fatih (Istanbul overview map top right corner)

Hollnagel et al. (2006), the plans do not take the effects from a changing environment with interrelated components into account sufficiently. As a result, potential disruptions caused by earthquakes can be overlooked and with that the existing plans can become unapplicable to the real situation. Thus, the **problem** is that static solutions are provided for a dynamic and complex environment (Hollnagel et al., 2006). This study focusses on

* Corresponding author

potential disruptions within traffic control which refers to operational procedures that guide the evacuation of vehicles and access of emergency services to and from disastrous areas. This needs to remain functional during an earthquake, making it essential to understand the causes of the potential disruptions to suggest measures that reduce the impact of earthquakes in such a dynamic environment.

This study analyses the potential disruptions that impact traffic control with the help of a multi-hazard risk assessment for the case study area Additionally, the use of 3D models for the visualisation of disaster risk is introduced. Redweik et al. (2017) stated that 3D models reduce the cognitive effort required to analyse the situation due to the multi-dimensionality. Thus, by using 3D models, environmental interactions should become more apparent which makes it possible to better understand and communicate the underlying causes of disruptions that impact traffic control and based on that suggest more dynamic solutions.

2. IDENTIFYING POTENTIAL DISRUPTIONS

In this study, three historical earthquake events were analysed to increase the understanding of how and what disruptions occurred. This is used to identify potential disruptions that could occur in the case study area. These events include the Tohoku earthquake that happened in Japan in 2011, the Kobe earthquake that also happened in Japan in 1995 and the Christchurch earthquake that happened in New Zealand in 2011.

During the Tohoku earthquake, widespread damage to buildings and roads, blocked roads by mud and debris and concerns about radiation made several areas inaccessible for emergency services. In addition, lack of gasoline made transportation more difficult. Human behaviour caused an increase in the use of the communication network, causing communication issues which made disaster coordination more difficult. Besides this, people started to move around by car which caused traffic congestions that obstructed the emergency services (Khazai et al., 2011).

The Kobe earthquake led to a lot of damage causing major expressways that connected Kobe with other parts of the country to become unusable. Consequently, Kobe's transportation system was at less than 5% of its normal capacity. Besides this, it meant that important access routes for emergency services and transportation of goods to impacted areas were lost. Contributing to this were the blockages on many narrow roads caused by debris and other infrastructural elements. Besides this, human behaviour contributed to a large number of abandoned cars and people leaving the city, causing traffic congestion which obstructed the emergency services (Iida et al., 2000).

During the Christchurch earthquake, extensive damage to the road networks, bridges and tunnels, especially caused by liquefaction, in combination with road blockages due to rock falls greatly obstructed the transportation of goods. Contributing to this, was the evacuation of people from major buildings. This behaviour caused traffic congestions throughout the city (Giovinazzi et al., 2011).

Based on these events in combination with the local characteristics of the case study area known from literature, it was identified that the area is likely prone to damage to the road network. Besides this, due to the vulnerable, densely constructed building stock, it is likely that narrow roads will be blocked with debris of the buildings. Fatih is also known to have traffic congestion, low-income newcomers and tourists who are expected to have low risk awareness and preparedness, and many businesses. Thus, as happened during the Christchurch earthquake, it is likely that there are many people who will evacuate in a chaotic manner which could cause traffic congestions. Contributing, are the major hospitals near the area which will attract many people. Lastly, it is likely that the behaviour of people will cause the communication networks to be overloaded, causing communication issues for the disaster management organisations as happened in Tohoku.

3. METHODS

3.1 Research Design and Input data

An overview of the workflow as applied in this study is shown in Figure 2. An overview of the input data is shown in Table 1.

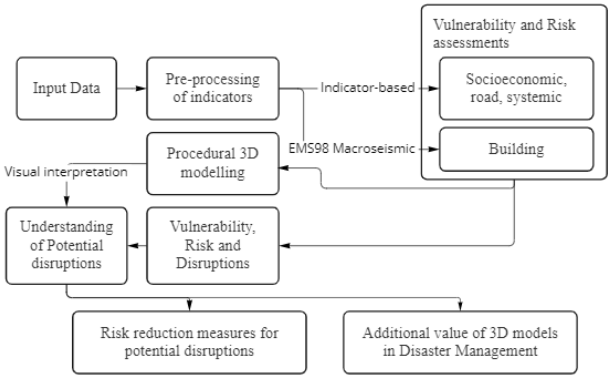

Figure 2. Research design of this study. Source: de Vries, 2022

Data	Type	Date	Source
Building and road footprints with semantic information e.g. building type and road width	.shp	2013	IMM[2]
Administrative boundaries of the case study area and Fatih	.shp	2013	IMM
Gender-based population and education-level per age group	.xlsx	2020	IPA[3]
Average day-time vehicle velocity and traffic intensity	.shp	2021	IMM
Buildings with additional semantic information e.g. construction year and height	.mdb	2018	IPA
Different types of facilities and road network within Faith	.shp	2015	TKGM[4]
Survey data about risk perception and income levels	.xlsx	2018	IPA
The peak ground acceleration (cm/s^2), fire distribution and liquefaction potential based on the worst-case scenario	.pdf	2002	(JICA & IMM, 2002)

Table 1. Overview of the input data. Source: de Vries, 2022

3.2 Vulnerability and Risk Assessments

The latest definition of disaster risk by the UNISDR's in 2017 is: 'the potential loss of life, injury, destroyed or damaged assets

[2] The Istanbul Metropolitan Municipality
[3] Istanbul Planning Agency
[4] The Land Registry and Cadastre of the Republic of Turkey

which could occur to a system, society or a community in a specific period of time, determined probabilistically as a function of hazard, exposure, vulnerability and capacity' (Schneiderbauer et al., 2017, p. 40). Disaster risk is not only about the probability and intensity of a hazard event, but also refers to the entities that are exposed and how vulnerable these are. For example, a severe earthquake in an area with very few people has less consequences than a minor earthquake in a highly populated area. As such, according to the Sendai disaster risk definition, risk exists of three components: hazard, vulnerability and exposure. The fourth component, coping capacity, is generally considered to be a part of vulnerability (Schneiderbauer et al., 2017). Consequently, risk can be determined according to Equation 1.

$$Risk = Hazard\ x\ Vulnerability\ x\ Exposure \quad (1)$$

In order to define these components, this study applied the additive normalisation indicator-based approach and the EMS-98 Macroseismic method (LM1) as proposed by the Risk-UE project (Milutinovic & Trendafiloski, 2003). The latter is adopted by e.g. Redweik et al. (2017). These approaches use indicators to represent the vulnerability and hazard of a community or area of interest. This study distinguishes between four categories in the vulnerability and risk assessments: physical road, physical building, socioeconomic and systemic. The **physical vulnerability** of buildings and roads, represents which of these are structurally weak (Banica et al., 2017), includes road and building typology, building age, height and use, difference in building height with adjacent buildings, building position in building block and road width and maintenance-level. **Social vulnerability** which represents characteristics of people and their situation that influence their ability to anticipate and resist the impact of disasters (Konukcu et al., 2015), includes population density, risk awareness, preparedness, people with low-education level (%), over 65 years old (%) and low-income level (%). **Systemic vulnerability** comprises the accessibility of emergency services to the disastrous areas and vice versa (Banica et al., 2017), and includes travel time to emergency facilities, solid to void ratio and traffic intensity. Throughout the study, these different assessments remained separated to be able to clearly distinguish between the types of vulnerability and risk that could cause a certain disruption.

3.3 Additive normalisation indicator-based approach

This method is applied to determine the road, socioeconomic and systemic vulnerability and risk. In order to be able to aggregate the selected indicators, they first need to be standardized into a small, specified, unitless range to remove the unit of measurement (Yoon, 2012). After this, the vulnerability and hazard indicators can be aggregated using equation 2.

$$Index = \sum_{i=1}^{n} w_i I_i \quad (2)$$

Where w_i = weight of the indicator
I_i = value of the indicator
n = the number of indicators

In this study, each indicator has equal weights, because this is most common according to Yoon (2012). After this, the vulnerability and hazard indices are multiplied according to Equation 1 to acquire the risk indices. Both the vulnerability and risk scores are standardized by applying the min-max rescaling technique (Equation 3). After this, the standardized vulnerability and risk values are categorized as shown in Table 2.

$$Y_i = \frac{X_i - X_{min}}{X_{max} - X_{min}} \quad (3)$$

where Y_i = standardized index
X_i = value of the index
X_{min} = lowest possible index
X_{max} = highest possible index

Vulnerability and risk indices	Classification
Index ≤ 0.25	Low
Index > 0.25 and Index ≤ 0.5	Medium
Index > 0.5 and Index ≤ 0.75	High
Index > 0.75 and Index ≤ 1	Very high

Table 2. Vulnerability and risk classes. Source: de Vries, 2022

3.4 EMS-98 Macroseismic method

This method is applied to determine the physical vulnerability and damage of the buildings in the case study area, because it defines the building typologies and damage grades with great quality. In this method, six vulnerability classes (A to F) of decreasing vulnerability are introduced. The method initially derives the vulnerability classes from the different building typologies: masonry, reinforced concrete (RC), wooden and steel buildings. Next to the typology of a building, it is possible that its vulnerability is affected by other structural characteristics which change its seismic behaviour. That is why, in this method Equation 4 has been introduced to determine an overall Vulnerability Index ($\bar{V}_i$) of a building based on its typology and the other related factors:

$$\bar{V}_i = V_i^* + \Delta V_r + \Delta V_m \quad (4)$$

Where $\bar{V}_i$ = vulnerability index
V_i* = typology vulnerability index
ΔV_r = regional vulnerability factor
ΔV_m = behaviour modifier factor

The building typology classification used in this study is shown in Table 3. The behaviour modifier factors that were considered according to the available data are shown in Table 4 and Table 5 These are summed to acquire the total behaviour modifier factor. The regional vulnerability factor, which can be used to alter the vulnerability indices based on expert judgement or historically observed vulnerability, was excluded in this study.

Building typology	Designation	V_i*
Steel	S1	0.363
Reinforced concrete	RC1	0.442
Wood	W	0.447
Masonry with RC slabs	M3.4	0.616
Masonry with wooden slabs	M3.1	0.74

Table 3. Building typology classes. Source: de Vries, 2022

Behaviour Modifier Factor	Option	V_m		
		Pre or Low code	Moderate code	High code
Age/code level		+0.16	0	-0.16
Number of stories	1-2 3-5 >6	-0.04 0 +0.08	-0.04 0 +0.06	-0.04 0 +0.04
Vertical Irregularity		+0.04	+0.02	0

Table 4. Behaviour Modifier Factors for RC buildings. Source: de Vries, 2022

Behaviour Modifier Factor	Option	V_m
Number of stories	1-2 3-5 > 6	-0.02 +0.02 +0.06
Vertical Irregularity		+0.02
Aggregate building: position	Detached Middle Header	0 -0.04 +0.06
Aggregate building: elevation[5]	1 2 3 4 5	-0.04 -0.02 0 +0.02 +0.04

Table 5. Behaviour modifier factors of other buildings. Source: de Vries, 2022

As presented by Milutinovic & Trendafiloski (2003), the calculated vulnerability indices can be correlated to a damage degree for a certain intensity scenario. This can be done using Equation 5. The results of this equation are rounded to agree with the Macroseismic damage scale which include five damage grades. The same approach is used by Redweik et al. (2017).

$$\mu_D = 2.5\left(1 + tanh\left(\frac{I + 6.25\bar{V}_i - 13.1}{2.3}\right)\right) \quad (5)$$

Where μ_D = damage degree
I = Macroseismic intensity
$\bar{V}_i$ = vulnerability index

(Bilal & Askan, 2014) determined the following relation (Equation 6) between the Peak Ground Acceleration (PGA) and the EMS-98 intensity scale based on their own database from Turkey.

$$I_{EMS-98} = 0.132 + 3.884\, log\, PGA_{max} \quad (6)$$

Where I_{EMS-98} = Macroseismic intensity
PGA_{max} = maximum peak ground acceleration (cm/s^2)

3.5 Road Closure Analysis

This study did a road closure analysis to define the risk for roads to be blocked by debris from buildings. It applied the same assumptions from the road closure analysis of Cakti et al. (2019) to determine this road closure risk: Completely damaged low-rise buildings (1-4 storeys) cause total closure in one-lane roads and partial closure in two-lane roads. Completely damaged mid-rise buildings (5-8 storeys) cause total closure in one- and two-lane roads and partial closure in three-lane roads. Completely damaged high-rise buildings (9-19 storeys) cause total closure in one-, two- and three-lane roads and partial closure in four-lane roads. One lane is considered 3m wide. This assumption is applied to buildings with damage grade 4 and 5, because these are considered completely damaged according to Milutinovic & Trendafiloski (2003). It is possible that buildings which are near each other create overlapping debris buffers. When this is the case, an increasing number of overlapping layers is assumed to represent an increasing likelihood of the debris to occur at that location and an increasing size of the debris making it less easy to remove

3.6 3D model creation

Visualisation of the vulnerability and risk using 3D modelling, as is the case in this study, has not been done extensively. Following the examples in the literature focusing on similar problems (e.g. Redweik et al. (2017)), and because of the ease of modelling operability, the possible combination with the commonly available GIS data and the potentially clear visual representation of the city and attributes, it was decided to use procedural modelling for this research.

Level of Detail 1 as defined by Kolbe (2009) was used considering the available data. Consequently, CGA rules are applied to extrude the building footprints based on their height information, to create textured roads, and to apply a green to red colour scheme representing low to high vulnerability and risk to both the buildings and the roads. Since the purpose of this study is to show which areas are more at risk and where potential disruptions are more likely to occur, visualising the vulnerability and risk using colours is considered more appropriate than realism. Lastly, debris is visualised in 3D by extruding the debris footprints and applying a white to red colour scheme depending on the number of overlapping footprints, representing the likeliness and size of the debris.

4. RESULTS

4.1 Vulnerability, Risk and Disruptions

4.1.1 Socioeconomic Vulnerability and Risk

The socioeconomic vulnerability as presented in Figure 3 is high or very high. Molla Gürani has a very high socioeconomic vulnerability. The reason Molla Gürani is more vulnerable than the other neighbourhoods can be attributed to the low risk awareness and risk preparedness in the neighbourhood.

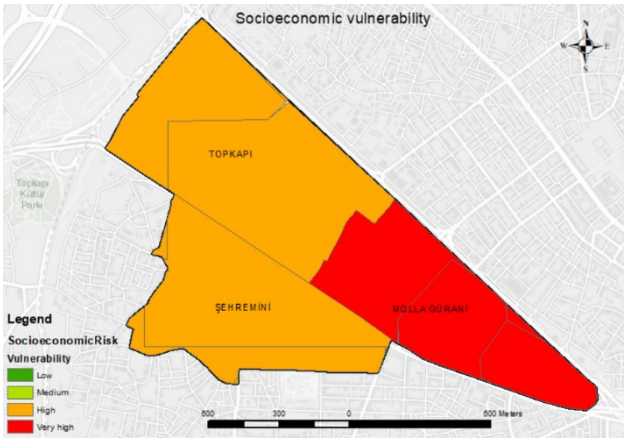

Figure 3. Socioeconomic vulnerability. Source: de Vries, 2022

The determined socioeconomic risk from combining the vulnerability with the hazards in the area i.e. the earthquake and cascading fires is shown in Figure 4. A significant part in Molla Gürani is shown to be at high socioeconomic risk. This can be attributed to its very high socioeconomic vulnerability in combination with the high risk to fire outbreaks. Next to this, a significant part of the neighbourhood Topkapi and small parts of the neighbourhood Sehremini are also shown to be at high risk.

[5] (1) Adjacent buildings are higher (2) An adjacent buildings is higher and another at the same level (3) Adjacent building have the same level (4) An adjacent buildings is lower and another at the same level or is higher (5) Adjacent buildings are lower.

This is caused by the increased fire outbreak potential and peak ground acceleration (400-500 cm/s^2) in those areas.

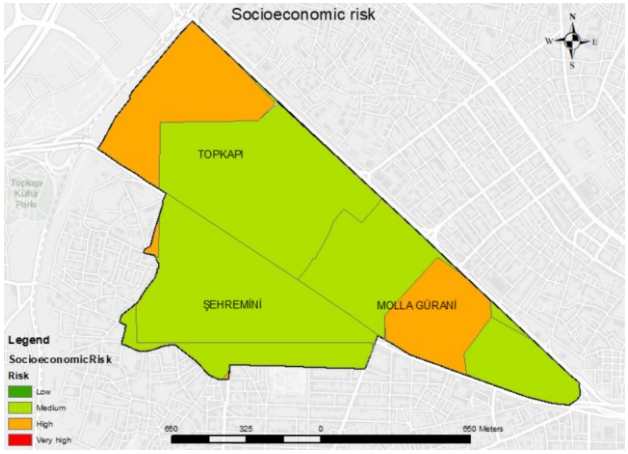

Figure 4. Socioeconomic risk. Source: de Vries, 2022

As described in Section 2, the behaviour of people was a recurring factor that contributed to the impact of the Tohoku, Kobe and Christchurch earthquakes by causing traffic jams and communication issues. It can be said that the unsuitable behaviour of people during an earthquake event is the result of their socioeconomic vulnerability including their risk awareness, preparedness, education level, etc. because this represents their knowledge on how to act and ability to act properly (e.g. elderly can be considered less mobile). With the high socioeconomic vulnerability in the area caused by such indicators unfitting behaviour can be expected.

As stated by the IMM, people are likely to move out of the dense area during an earthquake. According to the IPA, they will move to the coasts or stay in the neighbourhoods and move around by car. Consequently, it can be expected that there will be a lot of traffic on the main roads and within the neighbourhoods of the area, which will obstruct critical services in their activities.

Besides this, it is likely that the people who not only live in the area, but also in the rest of Istanbul, will use the communication networks to reach out to for example their families. As a result, it is likely that the phone services will collapse. This is also expected to be an issue according to the AFAD[6] and ITU[7]. It will cause difficulties for the emergency services since they will receive less information on the impacted areas from the disaster coordinating organisations. This might delay them in or even prevent them from operating properly.

4.1.2 Road Vulnerability and Risk

The road vulnerability as presented in Figure 5 shows that the main streets of the area (>9m wide) have low vulnerability. The reason for this is that they are made of strong material (paved with asphalt or parquet), maintained well and are significantly wide. The other streets have medium vulnerability. Like the main roads these are made of asphalt or parquet and are maintained well. Their higher vulnerability is caused by the narrow width of the streets. As such, it is more likely that the roads become impassable when these are damaged.

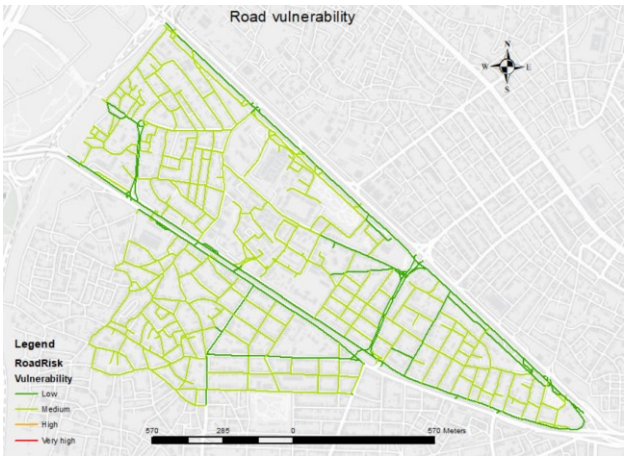

Figure 5. Road vulnerability. Source: de Vries, 2022

The road risk as presented in Figure 6 shows to be low for most part of the area. Roads with a width of less than 4m are at medium risk to damage. Also, roads with a width of 5 to 12m which are prone to high PGA levels (400-500 cm/s^2) are at medium risk. There is no (very) high risk to road damage in the area meaning that it is unlikely that the roads become impassable due to damage. Thus, it is expected that road damage will not disrupt the traffic control. According to the IPA this is expected, because the infrastructure is considered resilient against earthquakes.

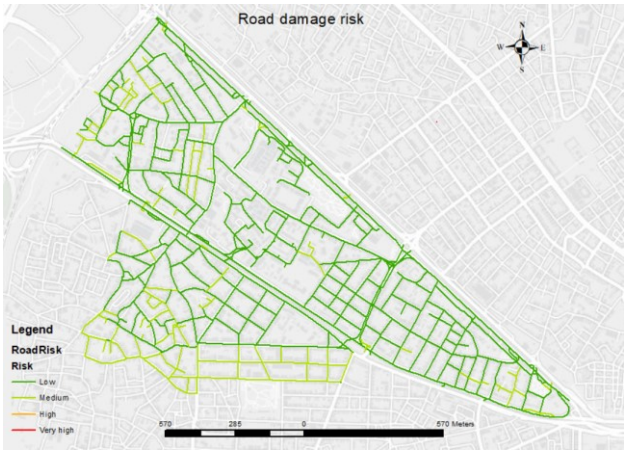

Figure 6. Road risk. Source: de Vries, 2022

4.1.3 Building Vulnerability and Damage Grades

The building vulnerability as presented in Figure 7 shows that 76.5% of the buildings have vulnerability class B or C. This is to be expected considering the fact that the area mostly exists of low-quality dwellings (Atun & Menoni, 2014). Most of the buildings with vulnerability level B are located in Molla Gürani. The largest component of buildings with vulnerability level C are located in Topkapi and Sehremini. Buildings with the other vulnerability levels are scattered throughout the area. As a result, the buildings in Molla Gürani can be considered most vulnerable.

The damage grades as presented in Figure 8 and Table 6 show that 89.2% of the buildings have damage grade 3 or 4. The statistics show that 66% of the buildings with damage grade 4 are masonry which are most prone to receiving damage with 87.1% of them having damage grade 4. RC buildings mainly receive damage grade 3 (57.3%). The RC buildings that received damage grade 4 are all buildings constructed before 1980 according to

[6] Disaster and Emergency Management Presidency

[7] Istanbul Technical University

low design standards. The other building typologies received damage grade 2.

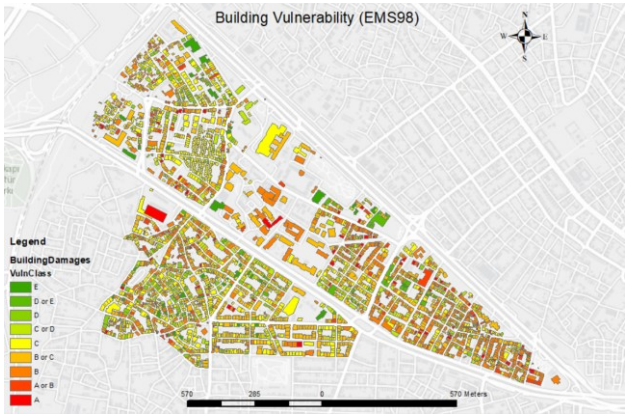

Figure 7. Building vulnerability. Source: de Vries, 2022

Almost half (43.8%) of the buildings with damage grade 4 are located in Molla Gürani, where also 21.8% of the buildings with damage grade 3 are located. Within the neighbourhood 65.4% of the buildings receive damage grade 4. In Sehremini 36.7% of the buildings with damage grade 4 and 44.5% with grade 3 are located. Both buildings with damage grades 3 and 4 are almost equally present. Only 19.4% of buildings with damage grade 4 and 33.6% with damage grade 3 are located in Topkapi. Within the neighbourhood 52.0% of the buildings show to receive damage grade 3. Based on this, it can be said that the buildings in Molla Gürani are most at risk to receiving building damage.

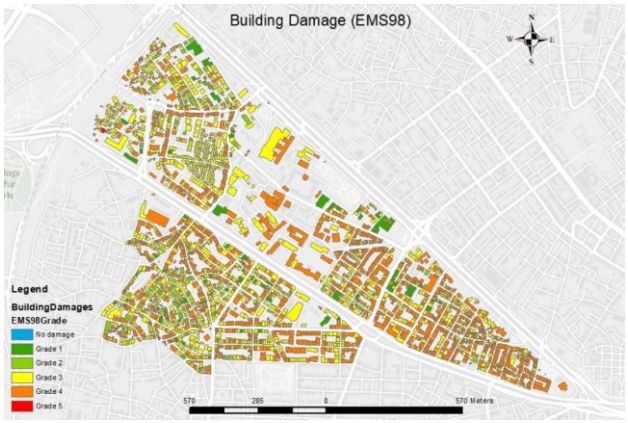

Figure 8. Building damage grades. Source: de Vries, 2022

Damage grade	**0**	**1**	**2**	**3**	**4**	**5**
Number of buildings per Building typology						
Reinforced concrete	0	131	251	1334	613	0
Masonry	0	0	0	176	1192	1
Wood	0	0	12	1	0	0
Steel	0	0	6	0	0	0
All	0	131	269	1511	1805	1
Number of buildings per Neighbourhood						
Sehremini	0	64	132	673	663	0
Topkapi	0	19	97	508	351	1
Molla Gürani	0	48	40	330	791	0

Table 6. Building damage statistics. Source: de Vries, 2022

Based on these results, the road closure analysis was done. The results as presented in Table 7 show that 43.2% of the roads are at (very) high road closure risk. These mainly include relatively narrow roads (<8m wide). As can be seen, the largest component of roads of 0-4m wide are at very high risk to road closure. Similarly, the largest component of roads of 5-8m wide are at low or very high risk to road closure. Wider roads are increasingly less prone to blockages, because their largest components are at low risk.

Width(m) / Risk	0-4	5-8	9-12	13-16	>16	All
Low	26	152	31	30	97	327
Medium	19	47	9	6	3	84
High	21	70	12	2	0	101
Very high	41	150	6	1	0	211

Table 7. Road closure risk statistics. Source: de Vries, 2022

Figure 9 shows that mainly the more narrow roads, especially in Molla Gürani and Sehremini, are prone to road closure which could prevent the emergency services to provide emergency aid, while the wider roads will remain accessible for the emergency services. This is as expected by the AFAD, ITU and fire brigade, who thought that road blockages by debris are very likely, because there are a lot of tall, densely constructed buildings near narrow roads.

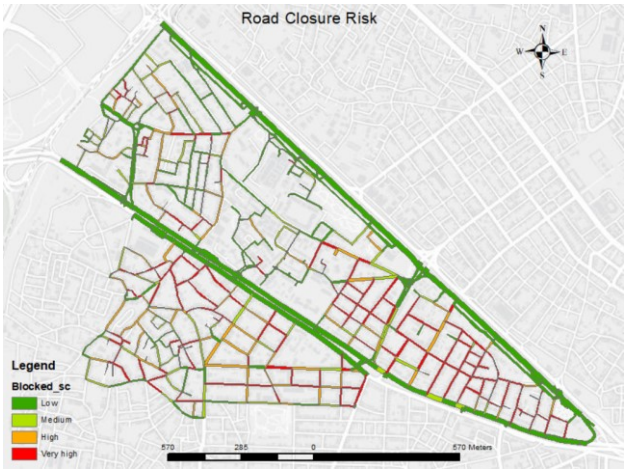

Figure 9. Road closure risk. Source: de Vries, 2022

4.1.4 Systemic Vulnerability and Risk

The systemic vulnerability as presented in Figure 10 shows that approximately half (49.2%) of the roads have a medium systemic vulnerability, while the rest has low systemic vulnerability. These are mostly present within the inner roads of Molla Gürani and Sehremini in addition to some parts of main roads. This can be attributed to the combination of a relatively long travel time to the fire brigades, traffic intensity and solid to void ratio. These factors reduce the accessibility to an area making it more likely that it will take the emergency services, especially the fire brigade, a relatively long time to reach the impacted areas.

The systemic risk as presented in Figure 11 shows that most parts within the area have low systemic risk with just 13.8% of the roads having medium risk. The higher systemic risk can be attributed to the distance to the liquefaction zones and the road closure risk in combination with a medium systemic vulnerability. These roads are mainly present in the south and southwest of the neighbourhood Sehremini and around the road in Molla Gürani that connects the two main roads of the area. These parts will be relatively more difficult and time-consuming to reach for emergency services during an earthquake event due to the likely increased traffic and potential road blockages.

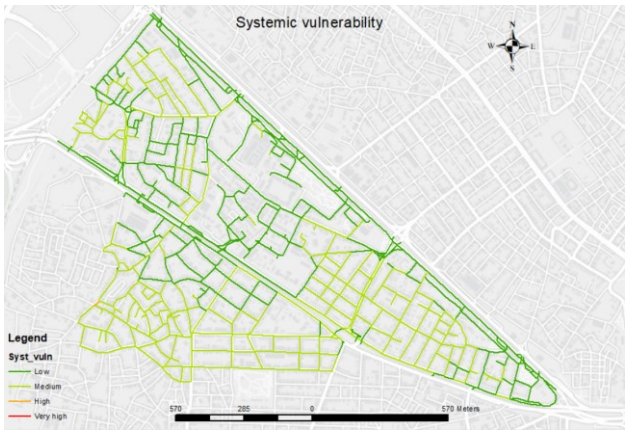

Figure 10. Systemic vulnerability. Source: de Vries, 2022

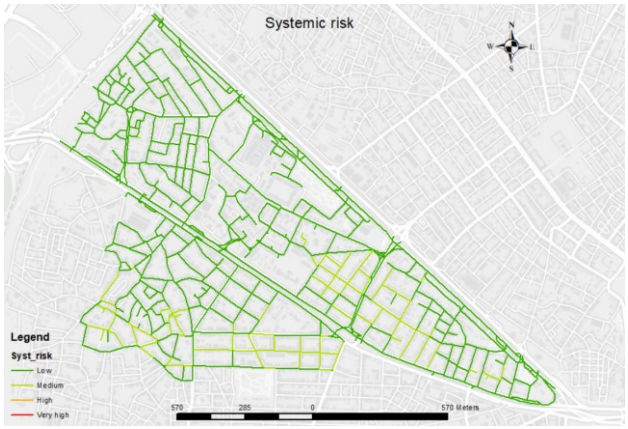

Figure 11. Systemic risk. Source: de Vries, 2022

4.2 Application of the 3D models

Visualisation of the building damage in 3D together with the road risk is shown in Figure 12. By visual interpretation, it becomes apparent that there are relatively high, densely built buildings which surround narrow streets and are expected to receive damage grade 3 or 4. Besides, the identification of buildings is improved since the different buildings are recognized easier by applying the height than in the 2D map as shown in Figure 8.

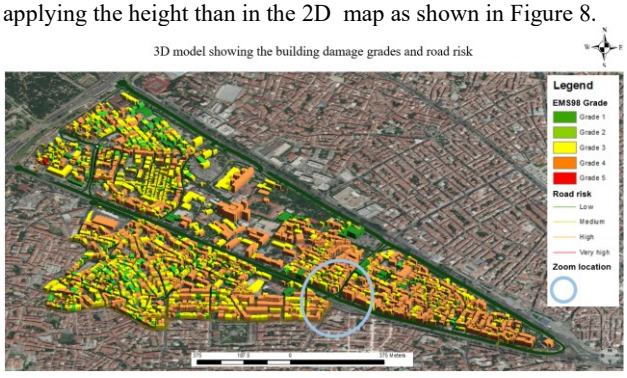

Figure 12. 3D model of the entire area. Source: de Vries, 2022

This especially becomes apparent when zoomed-in as is done in Figure 13. It clarifies that the narrow roads with (very) high road closure risk are usually surrounded by heigh, very heavily damaged buildings, while the major road does not show this risk, where the road is not entirely blocked by debris due to its width. Besides, the 3D models are more convincing in communicating that other potential disruptions, such as the occurrence of traffic jams, are realistic, because it is more apparent how dense the area actually is. To explore the 3D models further in the web scene the link in the caption of the Figure is provided.

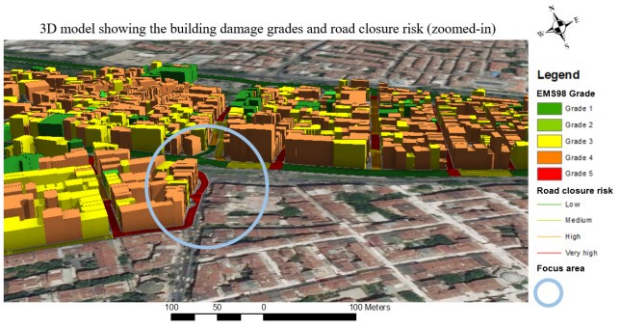

Figure 13. 3D model zoomed-in. Web scene: https://bit.ly/3KJiv7c . Source: de Vries, 2022

5. DISCUSSION

It is possible that there are other disruptions which were not identified during the analysis of the historical earthquake events. As such, it could be that there are additional potential disruptions, such as the loss of power systems, which can occur and affect the traffic control in the area. However, the identified disruptions are found to be most recurring in literature.

This study applied a limited number of indicators to determine the vulnerability and risk. In literature, additional indicators can be found for such assessments, e.g. the building maintenance and plan irregularity, soil type and road embankments. The use of a limited number of indicators could have affected the results of Section 4.1. However, the results show to be in line with JICA & IMM (2002), (Ugur et al., 2018) and Cakti et al. (2019).

Lastly, Redweik et al. (2017) suggests to use LoD2 for the 3D models which could for example increase the interpretation of the area. Consequently, the results might become more convincing and useful for the communication of disaster risk.

6. CONCLUSION

The results show that the roads are not vulnerable to damage. However, having debris from buildings will likely create damage and cause blockages. It was determined that 43.2% of the roads are expected to be blocked by debris. These mainly include narrow roads (<8m wide) located in Molla Gürani and Sehremini that are surrounded by a large number of 'very heavily damaged' buildings. Especially, Molla Gürani shows to be in danger of receiving significant building damage. The socioeconomic vulnerability is also shown to be high, especially in Molla Gürani. As a consequence, it is expected that inappropriate human behaviour such as chaotic evacuation and overloading the communication networks will cause traffic congestions and the communication issues between disaster management services to become problematic. All this contributes to the increased systemic risk in the south and southwest of the neighbourhood Sehremini and around the road in Molla Gürani that connects the two main roads of the area.

The additional value of including 3D modelling in disaster risk reduction is that it makes it easier to recognize the morphology of an area and that it contributes to the understanding and communication of the underlying causes of potential disruptions. This could help decision-makers in suggesting more local measures that mitigate the underlying causes of the potential disruptions and help disaster coordinating organisation in preparing more dynamic action plans.

ACKNOWLEDGEMENTS

The Authors are grateful for the provision of data by the IMM and IPA and the information by the spokespersons of the organisations that were consulted.

REFERENCES

Alpar, B., Alt, Y., Gazio, C., & Yücel, Z. Y. (2003). Tsunami Hazard Assessment in İstanbul. *Turkish J. Marine Sciences*, 9(1), 3–29.

Atun, F., & Menoni, S. (2014). Vulnerability to earthquake in Istanbul: An application of the ensure methodology. *A/Z ITU Journal of the Faculty of Architecture*, 11(1), 99–116.

Banica, A., Rosu, L., Muntele, I., & Grozavu, A. (2017). Towards urban resilience: A multi-criteria analysis of seismic vulnerability in Iasi City (Romania). *Sustainability 2017*, 9(2), 270. https://doi.org/10.3390/SU9020270

Bilal, M., & Askan, A. (2014). Relationships between Felt Intensity and Recorded Ground-Motion Parameters for Turkey. *Bulletin of the Seismological Society of America*, 104(1), 484–496. https://doi.org/10.1785/0120130093

Cakti, E., Safak, E., Hancilar, U., Sesetyan, K., Bas, M., Kilic, O., Yahya Mentese, E., Uzunkol, Ö., & Kara, S. (2019). İstanbul İli Olası Deprem Kayıp Tahminlerinin Güncellenmesi Projesi. In *BOUN - IMM*.

Ergintav, S., Reilinger, R. E., Cakmak, R., Floyd, M., Cakir, Z., Dogan, U., King, R. W., McClusky, S., & Ozener, H. (2014). Istanbul's earthquake hot spots: Geodetic constraints on strain accumulation along faults in the Marmara seismic gap. *Geophysical Research Letters*, 41(16), 5783–5788. https://doi.org/10.1002/2014GL060985

Giovinazzi, S., Wilson, T., Davis, C., Bristow, D., Gallagher, M., Schofield, A., Villemure, M., Eidinger, J., & Tang, A. (2011). Lifelines performance and management following the 22 February 2011 Christchurch earthquake, New Zealand: Highlights of resilience. *Bulletin of the New Zealand Society for Earthquake Engineering*, 44(4), 402–417. https://doi.org/10.5459/bnzsee.44.4.402-417

Hollnagel, E., Woods, D. D., & Leveson, N. (2006). *Resilience engineering : concepts and precepts* (1st ed.). CRC press. https://doi.org/https://doi.org/10.1201/9781315605685

Iida, Y., Kurauchi, F., & Shimada, H. (2000). Traffic Management System Against Major Earthquakes. *IATSS Research*, 24(2), 6–17. https://doi.org/10.1016/S0386-1112(14)60024-8

JICA, & IMM. (2002). Japan Internation Cooperation Agency (JICA) & Istanbul Metropolitan Municipality (IMM). *The Study on A Disaster Prevention / Mitigation Basic Plan in Istanbul including Seismic Microzonation in the Republic of Turkey* (Vol. 2).

Khazai, B., Daniell, J., & Wenzel, F. (2011). The March 2011 Japan Earthquake: Analysis of Losses, Impacts, and Implications for the Understanding of Risks Posed by Extreme Events. *TATuP - Zeitschrift Für Technikfolgenabschätzung in Theorie Und Praxis*, 20(3), 22–33. https://doi.org/10.14512/TATUP.20.3.22

Kolbe, T. H. (2009). Representing and exchanging 3D city models with CityGML. In J. Lee & S. Zlatanova (Eds.), *3D Geo-Information Sciences. Lecture Notes in Geoinformation and Cartography* (pp. 15–31). Kluwer Academic Publishers. https://doi.org/10.1007/978-3-540-87395-2_2

Konukcu, B. E., Menteşe, E. Y., & Kiliç, O. (2015). Assessment Of Social Vulnerability Against Disasters: A Pilot Case For An Earthquake In Istanbul. *WIT Transactions on The Built Environment*, 150, 13–24. https://doi.org/10.2495/DMAN150021

Milutinovic, Z. V., & Trendafiloski, G. S. (2003). WP4 Vulnerability of Current Buildings. In *RISK-UE Project Handbook*.

Redweik, P., Teves-Costa, P., Vilas-Boas, I., & Santos, T. (2017). 3D City Models as a Visual Support Tool for the Analysis of Buildings Seismic Vulnerability: The Case of Lisbon. *International Journal of Disaster Risk Science*, 8(1), 1–18. https://doi.org/10.1007/s13753-017-0141-x

Schneiderbauer, S., Simmons, D. C., Corbane, C., Menoni, S., & Zschau, J. (2017). Understanding disaster risk: risk assessment methodologies and examples. In K. Poljanšek, M. Marin Ferrer, T. De Groeve, & I. Clark (Eds.), *Science for disaster risk management 2017: knowing better and losing less.* (pp. 40–119). Publications Office of the European Union. https://doi.org/10.2788/688605

Shimizu, M., & Clark, A. L. (2015). Interconnected Risks, Cascading Disasters and Disaster Management Policy: A Gap Analysis. *GRF Davos Planet@Risk*, 3(2), 260–270.

Ugur, C., Ugur, C., Güzelkaya, D., Ohran, A., Kalaycioglu, S., Çelik, K., Türkyilmaz, S., Çelen, Ü., Mentese, E. Y., Kara, S., Kilic, O., & Bas, M. (2018). İstanbul ili genelinde afetler karsisinda sosyal hasar görebilirlik analizi icin anket calismasi isi. In *Istanbul Büyüksehit Belediyesi, Deprem ve Zemin İnceleme Müdürlüğü'ne aittir*.

Yoon, D. K. (2012). Assessment of social vulnerability to natural disasters: A comparative study. *Natural Hazards*, 63(2), 823–843. https://doi.org/10.1007/s11069-012-0189-2